Microwave mixing in microbridges made from $YBa_2Cu_3O_{7-x}$ thin films

K. S. Il'in[a] and M. Siegel
Institut für Schichten und Grenzflächen, Forschungszentrum Jülich GmbH, Jülich 52425, Germany

(Received 21 February 2002; accepted for publication 8 April 2002)

We present a systematic study of the response of a $YBa_2Cu_3O_{7-x}$ thin-film microbridge to millimeter wave radiation. The dependencies of the microwave response spectrum on the bias voltage and operating temperature have been measured on samples made from $YBa_2Cu_3O_{7-x}$ films with different thicknesses. Once the bias voltage exceeds the value corresponding to the first maximum of differential resistance, the value of the -3 dB roll-off frequency of the microbridge response is drastically reduced. On the other hand, at temperatures close to T_c the roll-off frequency rises to about 20 GHz. For high resistivity $YBa_2Cu_3O_{7-x}$ films with relatively low upper critical magnetic fields the -3 dB roll-off frequency is about 7 GHz even at temperatures much smaller than T_c. To explain the results obtained we consider the presence of two additive mechanisms that contribute to the $YBa_2Cu_3O_{7-x}$ thin-film microbridge response to microwave radiation: vibration of magnetic vortices and heating of electrons and phonons. The competition between these two mechanisms defines the bias voltage and temperature dependencies of the -3 dB roll-off frequency as well as the recently reported dependence of the intermediate frequency bandwidth of $YBa_2Cu_3O_{7-x}$ hot-electron bolometer mixers on the local oscillator frequency. Numerical calculations based on this assumption are in a good qualitative agreement with the experimental results. © *2002 American Institute of Physics.* [DOI: 10.1063/1.1481773]

I. INTRODUCTION

High-temperature superconductors (HTS) like $YBa_2Cu_3O_{7-x}$ (YBCO) were introduced recently as promising materials for the development of ultrafast sensitive heterodyne receivers of electromagnetic radiation.[1] One clear advantage of HTS is the high critical temperature of the superconducting transition, which exceeds the boiling temperature of liquid nitrogen. The operating temperature of HTS devices for most applications is higher than 20 K and it allows one to use low power cryocoolers, which is very significant for long-term atmospheric or space missions. With regard to YBCO thin films it is important to note another advantage of HTS. The very short inelastic electron-phonon scattering time $\tau_{\text{e-ph}} \approx 2$ ps at temperatures of about $T \approx 85-90$ K allows one to suggest YBCO thin films for the development of hot-electron bolometer (HEB) mixers of electromagnetic radiation with a characteristic -3 dB roll-off frequency f_{ro} up to 100 GHz.[2–5] This wide intermediate frequency (IF) bandwidth of the mixer is very important especially in the terahertz frequency range because of the lack of a tunable local oscillator (LO) for these frequencies. However, as shown in Ref. 1 the significant magnitude of the thermal boundary resistance of the YBCO film–substrate interface[6] limits f_{ro} of these devices to much smaller values of about 2–3 GHz. Moreover, recently[7,8] it has been demonstrated that mixers made from YBCO films have properties that are very different in comparison with theoretical estimates[1] and similar devices made from low-temperature superconductors. Li *et al.*[7] have obtained on 100 nm thick YBCO films a response spectrum with a roll-off frequency of about 9 GHz measured at 115 GHz LO frequency f_{LO} and a smaller value of 7 GHz at $f_{\text{LO}} = 585$ GHz (the operating temperature in both cases was about 70 K). Measurements performed in the radiation frequency range of 10–480 GHz have also shown a reduction of f_{ro} with an increase in photon energy[8] but much more considerably than that in Ref. 7. Also Harnack *et al.*[8] reported in that f_{ro} strongly depends on the bias voltage and changes from about 2 GHz for low-voltage bias operation down to hundred megahertz with an increase in bias voltage. Recently, in the range from 1 up to 20 GHz of radiation frequency the strong temperature dependence of f_{ro} has been observed mostly due to the shift of optimal operation points of the HEB mixer toward lower bias voltage as the temperature approaches T_c.[9] At operating temperatures much lower than the critical temperature the magnitude of f_{ro} was only several hundred megahertz for films with thickness $d = 30$ nm and increased up to 2.4 GHz at $T \approx T_c$.

To gain better insight into the physical processes responsible for the above mentioned features of YBCO HEB mixers we have performed a detailed systematic study of the response of YBCO thin-film microbridges to millimeter wave radiation over a wide temperature range and at different bias conditions. Based on the experimental results obtained we have assumed that the response of YBCO thin-film microbridges is due to contributions from two different mechanisms. Heating of electrons and phonons in the film mostly defines a response spectrum at temperatures much lower than T_c and bias voltages U_{bias} higher than voltage U_0, which corresponds to the first maximum of differential resistance (FMDR). The second mechanism is based on vibrations of magnetic vortices under the influence of external electromagnetic radiation. This mechanism dominates the response of

[a]Electronic mail: k.ilin@fz-juelich.de

YBCO microbridges at bias voltages lower than U_0, especially at temperatures close to T_c. The competition between these two mechanisms determines the magnitude of the microbridge response, its spectrum, the -3 dB roll-off frequency dependencies on the bias voltage, the operating temperature, and the local oscillator frequency.

This article is organized in the following way: In Sec. II we describe the technology for fabricating YBCO thin films and samples, their characteristics, and the experimental technique for measurement of the microwave response of the microbridges. The results of measurements of the response of YBCO thin-film microbridges at different bias voltages and a discussion of f_{ro} dependence on U_{bias} are presented in Sec. III. The experimental dependencies of the -3 dB roll-off frequency on the operating temperature and an analysis of processes in YBCO thin-film microbridges under millimeter wave radiation are presented in Sec. IV.

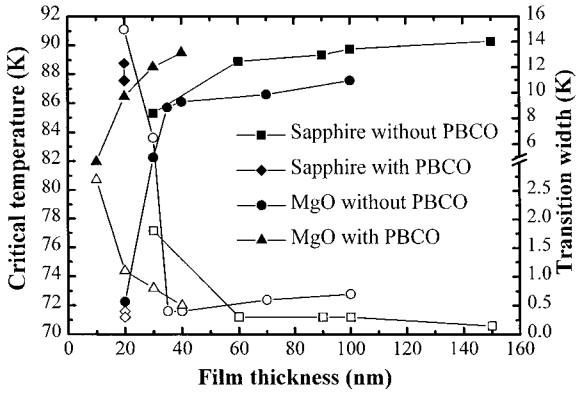

FIG. 1. Dependence of critical temperature T_c (closed symbols) and transition width ΔT (open symbols) on YBCO film thickness d for films deposited on MgO and sapphire substrates with and without a PBCO buffer layer. The lines are to guide the eye.

II. FABRICATION AND CHARACTERIZATION OF SAMPLES: EXPERIMENTAL TECHNIQUE

YBCO films with thicknesses from 10 to 100 nm were fabricated using the standard pulsed-laser deposition (PLD) technique. The density of the laser energy on the target was about 1 J/cm^2 per pulse and the repetition frequency of the laser pulses was 10 Hz. The substrates were commercially available single-side polished MgO (100) and sapphire (1102) single crystals with thicknesses of 0.3 and 0.5 mm, respectively. The substrates were glued on to the heater using silver paste for better thermal contact. The base pressure in the chamber was better than 5×10^{-5} mbar. For fabrication of YBCO films on sapphire substrates we used a CeO_2 buffer layer deposited *in situ* at a heater temperature of 820 °C and an oxygen pressure of $p_{O2}=0.2$ mbar. After deposition of CeO_2 we changed the target without breaking vacuum and deposited a YBCO film thicker than 20 nm at 810 °C and $p_{O2}=0.5$ mbar. For fabrication of YBCO films thicker than 40 nm on MgO substrates a 10 nm seed layer of YBCO was deposited at 650–780 °C and afterwards the residual thickness of YBCO was deposited at a higher temperature of 785 °C. The oxygen pressure of 0.5 mbar was kept constant during the whole process. Usually, YBCO films on MgO substrates with a seed layer deposited at higher temperature show a higher critical temperature T_c in comparison with films fabricated on seed layers, which have been grown at lower temperature. The width of the superconducting transition, ΔT, was approximately the same for all deposition temperatures of the seed layer. However, the long-term stability of superconducting characteristics (T_c and ΔT) was better in the case of low-temperature growth of the YBCO seed layer. The best combination of high T_c, narrow ΔT, and long-term stability was obtained for seed layers deposited at 700 °C. At these conditions typical values of $T_c\approx85$ K and $\Delta T\approx0.3$ K without any degradation for 3 months were obtained for YBCO films with a total thickness of 40 nm. A gold protective layer of about 50 nm thick was deposited *in situ* using dc-magnetron sputtering. After film fabrication the critical temperature and the width of the superconducting transition were measured using an inductive technique. The dependencies of T_c and ΔT on the total YBCO film thickness d are shown in Fig. 1 by closed (T_c) and open (ΔT) circles (YBCO films on MgO) and by squares (YBCO films on sapphire).

The technology described above is not applicable for YBCO films with thicknesses less than 40 nm. The 30 and 20 nm thick YBCO films on MgO show a strong reduction of T_c down to 82 and 72 K, respectively, along with abrupt broadening of the superconducting transition from $\Delta T=6$ K for thicker films to 15 K for the thinner ones (see Fig. 1). Additionally, these film shown strong degradation up to a total suppression of T_c with in a week of deposition. The strong lattice mismatch plays the major role in this situation. The top part of a YBCO film has a good and stable enough stoichiometric structure until the film thickness is more than the length of the lattice constant transition from MgO to YBCO. In this case T_c and ΔT have more or less monotonic dependence on the film thickness. For films with $d\leqslant30$ nm the lattice mismatch between the film and substrate already dominates over the whole film thickness. This is one reason for oxygen deficiency, which leads to a reduction of T_c and broadening of the superconducting transition. To avoid these effects for films with thicknesses less than 40 nm we developed a more complicated technological process. To improve substrate–film matching we deposited an additional $PrBa_2Cu_3O_{7-x}$ (PBCO) buffer layer using the same PLD technique. PBCO is a semiconductor with a crystalline structure[10] similar to that of YBCO and the lattice mismatch between these two materials is negligible ($\leqslant$1.5%). The PBCO buffer layer with a thickness of about 20 nm was deposited directly on to the MgO substrate at a temperature of 780 °C and oxygen pressure of 0.4 mbar. Then we deposited the YBCO film at 795 °C and $p_{O2}=0.5$ mbar. For fabrication of YBCO films thinner than 30 nm on sapphire substrates, first we deposited a CeO_2 buffer layer, then a 20 nm thick PBCO layer at 810 °C and $p_{O2}=0.5$ mbar and, after that, the YBCO film. Finally, we deposited a thin PBCO film ($\approx$10 nm) on top of the YBCO film. This second PBCO layer was used as a protective layer for the YBCO film during ion beam etching. Moreover, our experience shows that YBCO films with a PBCO protective layer are more stable than YBCO films, which have not been covered by PBCO.

TABLE I. Parameters of the samples.

Sample	T_c (K)	ΔT (K)	R_n (100 K) (Ω)	d (nm)	Substrate	j_c (40 K) (A/cm^2)
Sp2 No. 11	85	9	336	20	Sapphire	1×10^7
Sp2 No. 17	81	16	706	20	Sapphire	2.2×10^6
MgO4 No. 3	87.8	3.6	81	100	MgO	2.2×10^7
MgO4 No. 5	87.6	2.8	34	100	MgO	2.4×10^7
MgO3 No. 11	72	19	257	40	MgO	5.75×10^5
P348 No. 13	87.85	4.3	137	90	Sapphire	2.9×10^6
MgO17 No. 10	77.4	9	37.6	20	MgO	2.6×10^6

Figure 1 shows the dependence of T_c and ΔT (closed and open triangles, respectively) of YBCO films on MgO with a PBCO buffer layer on YBCO film thickness d. It is seen that even for the thinnest film with $d=10$ nm a transition temperature of $T_c\approx82$ K is still higher than the liquid nitrogen temperature and that $\Delta T\approx2.8$ K is smaller than even that for 30 nm thick YBCO films deposited on MgO without a PBCO buffer layer. We also deposited several YBCO films with $d=20$ nm on a sapphire substrate with a PBCO buffer layer. For these films $T_c\approx88$ K and $\Delta T\approx0.4$ K measured just after film fabrication are shown in Fig. 1 by closed and open diamonds. However, over a few days these films degraded and after stabilization of the film characteristics we found $T_c\approx84$ K and $\Delta T=1.5$ K. These parameters are a little bit worse than those of the YBCO film with the same thickness on MgO with a PBCO buffer layer.

The YBCO films were patterned into microbridges with width ≈1 μm and length ≈1.5 μm limited by gold contact pads using standard photolithography and the ion-beam etching technique. After patterning, a 100 nm thick SiO layer was thermally evaporated on top of the bridge to protect it against mechanical damage and absorption of water. The superconducting and dc parameters of the samples discussed in this article, measured by a standard four-probe method, are listed in Table I. The superconducting transition width was determined as $\Delta T=T_c$on$-T_c$off, where $T_c$on and $T_c$off correspond to 0.9 and $0.1R_n$, respectively (R_n is the resistance of a sample in the normal state). The critical temperature was taken in the middle of transition. The current according to a voltage drop of 50 μV was defined as the critical current I_c.

For YBCO film characterization we also measured the temperature dependence of the second critical magnetic field $H_{c2}(T)$ of several samples. In these measurements a sample was mounted on a copper block near the temperature sensor. An external magnetic field perpendicular to the YBCO film surface was created by a 2 T superconducting solenoid mounted on a standard Heliox 2VL insert (Oxford Instruments).[11] At temperatures near T_c we determined a magnitude of the magnetic field, at which the resistance of a sample reached a value of about $0.2R_n$. This value of the magnetic field we related to the second critical magnetic field at given temperature of $H^*_{c2}(T)$. Of course, the magnetic field determined in this way is not the true value of H_{c2}, and we cannot calculate the absolute magnitude of $H_{c2}(0)$. But based on the results we can obtain information about the relative difference between the $H^*_{c2}(0)$ of our different samples. For example, for samples Sp2 No. 11 and Sp2 No. 17 we have obtained approximately the same value of $H^*_{c2}(0)$ of about 26.5 T and for sample MgO4 No. 5 a two times larger magnitude of $H^*_{c2}(0)=57$ T.

Figure 2 shows a sketch of the experimental setup for measurements of the response upon electromagnetic radiation of YBCO thin-film microbridges. In our experiment we used two millimeter-wave generators: a tunable backward wave oscillator (BWO) with radiation frequency in the range of 78–119 GHz and a 90–94 GHz Gunn oscillator. The radiation frequency of the Gunn oscillator was fixed and the BWO was tuned in the range of intermediate frequency Δf from 1 MHz up to 25–30 GHz. The radiation from both sources was coupled to a device by a waveguide dipstick. In the course of measurements the sample was mounted on a copper holder along with a temperature sensor. One contact pad of the sample was grounded and the other was connected to a semirigid coaxial cable. The sample holder was attached to the output of the 3 mm waveguide dipstick, which was immersed into a liquid helium transport Dewar. The superconductivity in the sample was strongly suppressed by radiation from the BWO, which acts as a local oscillator in our experiment. The radiation power from the Gunn oscillator (signal source) was adjusted to be less than 1% of the power of the LO in order to avoid any influence of signal power on the operating point of the device. During measurement the radiation from the signal source and LO was kept constant. The sample was biased by a constant voltage source via a broadband bias tee. By altering the distance between the sample and the liquid-helium bath we changed the operating

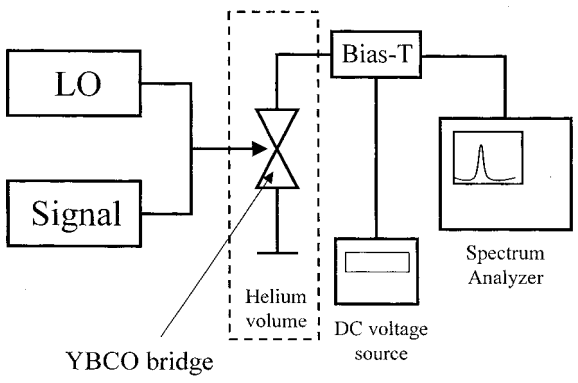

FIG. 2. Sketch of an experimental setup for measurements of the intermediate frequency spectra of YBCO thin-film microbridges. The local oscillator (LO) is a 78–119 GHz backward wave oscillator and the signal source is a 90–94 GHz Gunn oscillator.

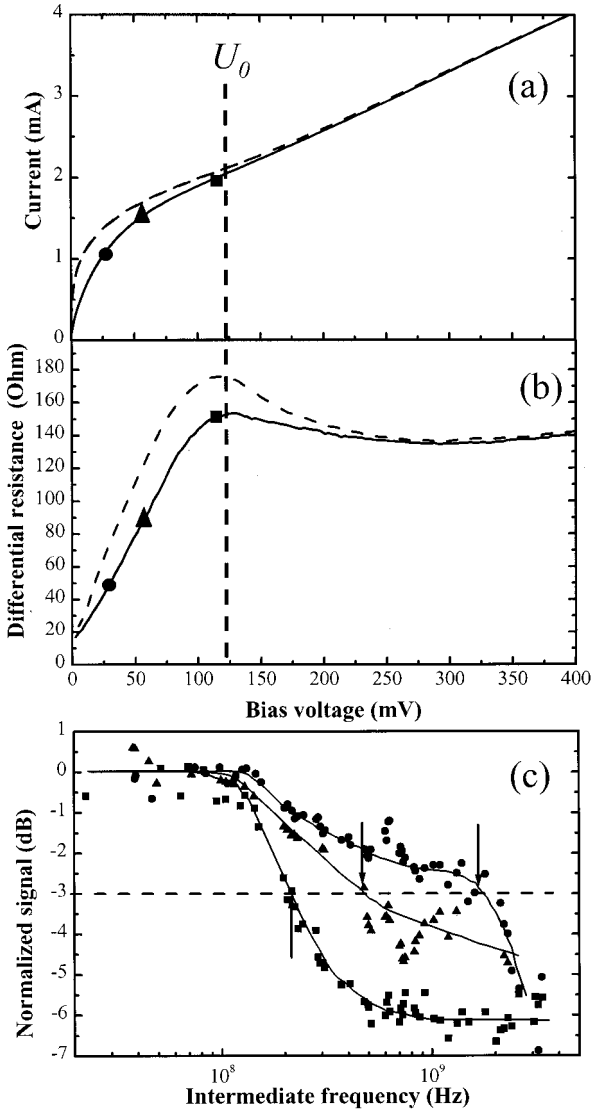

FIG. 3. (a) *IV* curves of sample MgO4 No. 3 at operation temperature $T=89.5$ K; dashed line: without irradiation, solid line: under optimal LO power; (b) differential resistance of the sample: dashed line: without irradiation; solid line: under LO power. The dashed vertical line shows the position of the bias voltage U_0 that corresponds to the first maximum of the differential resistance; (c) IF spectra measured at three bias voltage values; the dashed horizontal line shows the -3 dB level of the response drop, arrows indicate the position of f_{ro}. The solid lines are to guide the eye.

temperature, which was stable enough to measure a spectrum of the response of the sample in the whole IF range. The IF response of the sample was analyzed by a spectrum analyzer (Tektronix 2782) and automatically stored in a computer. The spectra measured were corrected, taking into account the losses of the IF power in the readout system.

III. −3 dB ROLL-OFF FREQUENCY DEPENDENCE ON THE BIAS VOLTAGE

Typical response spectra of a YBCO thin-film microbridge measured at different bias voltages are shown in Fig. 3(c) along with current–voltage characteristics [*IV* curves, Fig. 3(a)] and the dependence of the differential resistance dU/dI on the bias voltage [*dRV* curves, Fig. 3(b)] under

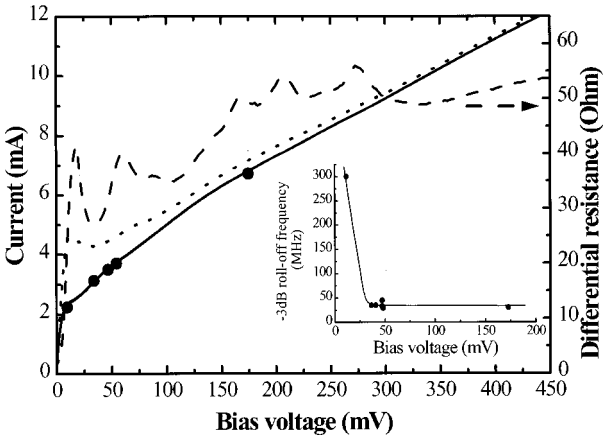

FIG. 4. *IV* curves of 100 nm thick YBCO microbridge (MgO4 No. 5) at $T=81.4$ K under LO power (solid line) and without irradiation (dotted line). Circles are operating points. The dashed line represents the dependence of differential resistance on the bias voltage. Inset: Bias voltage dependence of -3 dB roll-off frequency f_{ro}. The solid line is to guide the eye.

optimal LO power (solid lines) and without irradiation (dashed lines). The symbols on the *IV* and *dRV* curves indicate the operating points, at which the dependencies of sample response on intermediate frequency were measured. In these measurements at each bias voltage the LO power was adjusted in order to drive the sample into an optimal state, where the response from the sample is maximal. A dashed horizontal line shows the -3 dB level of the drop in response and arrows indicate the position of the -3 dB roll-off frequency f_{ro} in Fig. 3(c). It is clearly seen in Fig. 3(c) that the shape of the spectrum and the magnitude of f_{ro} are essentially dominated by the value of the bias voltage. The spectrum measured at the highest bias voltage (shown by squares) has the steepest dependence of microbridge response on the intermediate frequency and at the same time the smallest magnitude of -3 dB roll-off frequency. The spectrum measured at the bias voltage indicated in Figs. 3(a) and 3(b) by circles is characterized by the flattest dependence of the response on IF. At this bias voltage the f_{ro} value is about an order of magnitude higher than it was at the highest bias voltage. The -3 dB roll-off frequency of the spectrum measured at intermediate bias voltage [triangles in Fig. 3(c)] is lower than f_{ro} of the low-voltage spectrum (circles) and higher than f_{ro} obtained at the highest U_{bias} (squares).

From the analysis of the dependence of the differential resistance on the bias voltage we have found that the shape of the spectrum and the f_{ro} value correlate with the position of the operating point on the *IV* curve with respect to the FMDR. In Figs. 3(a) and 3(b) a vertical dashed line shows the position of the FMDR on the *IV* and *dRV* curves. The corresponding voltage will be denoted by U_0. In a first approximation, we divide the whole range of bias voltage into two ranges separated by voltage U_0. For sample MgO4 No. 3 (see Fig. 3) all operating points are at $U_{bias} \leqslant U_0$, nevertheless the closer the operating point to FMDR the smaller value of f_{ro}. However, results obtained on a similar sample (MgO4 No. 5) show rapid changes of the f_{ro} value at bias voltage equal to U_0. In Fig. 4 we present the *IV* and *dRV* curves of this sample along with the f_{ro} dependence on the

bias voltage in the inset. Only one operating point for this device is at $U_{bias}<U_0$, all others are at voltages higher than U_0. For the low-voltage operating point we have obtained f_{ro} of about 300 MHz (see the inset in Fig. 4). For all operating points at $U_{bias}>U_0$ the value of f_{ro} is almost constant and is about one order of magnitude smaller ($\approx$35 MHz) than f_{ro} obtained at bias voltage of $U_{bias}<U_0$. This result was obtained on sample MgO4 No. 5 at $T=81.4$ K, which is noticeably lower than the critical temperature. The *IV* curve measured without LO power (dotted line in Fig. 4) has a peak of the current at low voltages, which clearly indicates the presence of self-heating of the sample and the formation of a hot spot inside the YBCO bridge. The differential resistance of the irradiated sample has at least five clear observable maxima in its dependence on bias voltage (dashed line in Fig. 4). However, the value of f_{ro} after the FMDR remains the same independent of the position of the operating point, whether it is just after the FMDR or at voltages higher than U_{bias}, which corresponds to the second or third maximum on the *dRV* curve. Generally, all samples investigated demonstrate similar influence of the bias voltage on the -3 dB roll-off frequency.

Based on the experimental results we can formulate this phenomenon in the following way: at voltages lower U_0 the -3 dB roll-off frequency of the photoresponse of the YBCO thin-film microbridge has a larger value than at $U_{bias}>U_0$. At $U_{bias}\leqslant U_0$ the f_{ro} value decreases more or less monotonically as the bias voltage approaches U_0.

Note that the value of U_0 is different for different samples ($\approx$125 mV for MgO4 No. 3 and $\approx$17 mV for MgO4 No. 5) and depends slightly on the operating temperature. The position of the FMDR shifts toward higher bias voltage with an increase in temperature. For example, for sample Sp2 No. 17 we have found that U_0 at 75 K is about 1.3 times larger than at $T=7.4$ K. At the same time the second and other peaks on the *dRV* curves shift toward lower U_{bias} as the operating temperature increases.

The presence of the peaks on the *dRV* curve indicates the formation of one or several normal conducting regions with $T\geqslant T_c^*$ inside the YBCO bridge. The formation of a normal region occurs in the part of the bridge where the superconductivity is weaker, i.e., where the transition temperature T_c^* is lower than the average transition temperature of the microbridge. The presence of several maxima indicates that the increase of U_{bias} leads to series formation of some normal islands inside the bridge. Another possible explanation of this behavior of the differential resistance is the step by step expansion of the initial normal-state island due to joining of the neighboring parts of the microbridge. Additionally, each normal part increases due to Joule heating.

The values of f_{ro} measured at $U_{bias}>U_0$ correspond to the frequencies determined by the rate of the nonequilibrium phonons' escape from the YBCO film to the substrate $f_{es}=(2\pi\tau_{es})^{-1}$, where $\tau_{es}=100\times d$ (nm) ps for sapphire and $\tau_{es}\approx 49\times d$ (nm) ps for the MgO substrate.[6] The experimentally determined and calculated values of f_{es} are listed in Table II. The drop of the IF response due to phonon escape could be detected also at $U<U_0$. In this case the difference between the phonon escape plateau and the next one usually was less than 3 dB. But under certain conditions (one of them is relatively low temperature) it was enough to determine f_{es} via fitting of the low-frequency part of the spectrum using the following frequency dependence of the photoresponse:[12]

$$\Delta U_{es}(\Delta f)=\frac{\Delta U_{es}(0)}{\sqrt{1+(\Delta f/f_{es})^2}}. \tag{1}$$

The good agreement between the experimental and calculated values of f_{es} allows us to assert that the response spectrum measured at voltages higher than the voltage of the FMDR is dominated by electron-energy relaxation processes via inelastic electron–phonon interaction and phonon escape from the film to the substrate.[13]

At $U_{bias}<U_0$ and under LO irradiation the current is proportional to $\sqrt{U_{bias}}$ for most of the samples. This dependence of the current is typical of viscous motion of the magnetic vortices under Lorenz force.[14] Thus, we assume that at voltages lower than the voltage corresponding to the FMDR vortex motion dominates the dynamic properties of the YBCO thin-film microbridge.

TABLE II. Calculated and experimental values of the -3 dB roll-off frequency corresponding to the phonon escape from YBCO films to MgO and sapphire substrates.

Substrate	Film thickness (nm)	Calculated f_{es} (MHz)	Experimental f_{es} (MHz)
Sapphire	20	80	80
Sapphire	90	18	40
MgO	20	164	180
MgO	40	82	Not measured
MgO	100	29	33

IV. TEMPERATURE DEPENDENCE OF THE -3 dB ROLL-OFF FREQUENCY

Here we analyze the temperature dependence of the -3 dB roll-off frequency measured on the same samples. At $U_{bias}>U_0$ the experimental value of f_{ro} is dominated by phonon escape from the film to the substrate and has no essential dependence on T, which agrees with theory.[13] In the following discussion we will consider results obtained at bias voltages of $U_{bias}<U_0$. Within this voltage range the LO power and U_{bias} were adjusted to reach the maximum response of the sample. This adjustment was done at low T, after that the bias voltage was kept constant and at higher temperature we changed only the LO power to reach the maximal signal value. Three spectra measured on sample MgO3 No. 11 at different temperatures are shown in Fig. 5. Arrows indicate the position of the -3 dB drop of the signal on the curves related to operating temperatures of 40 and 66 K. The signal measured at $T=71$ K has no clearly detectable -3 dB drop even at the highest intermediate frequencies. A similar change in the response spectrum of the YBCO thin-film microbridge with an increase in operating temperature was obtained for all samples studied. In Fig. 6 we plot the temperature dependencies of f_{ro} for the samples discussed in this article. Usually at temperatures much lower than the critical

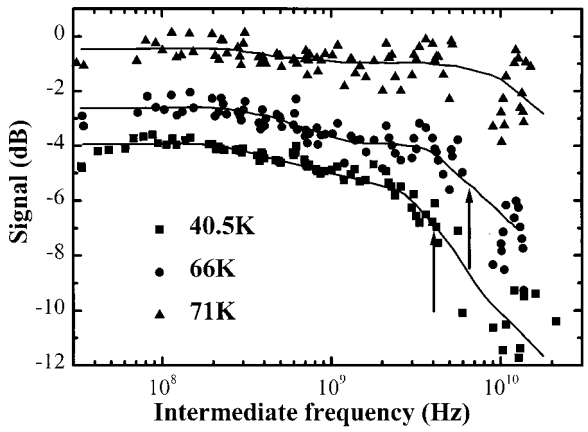

FIG. 5. Dependence of the response of a YBCO microbridge (MgO3 No. 11) on intermediate frequency at different operating temperatures measured at $U_{\rm bias}<U_0$. Arrows indicate the -3 dB drop of the signal. The lines are to guide the eye.

temperature the value of $f_{\rm ro}$ is weakly dependent on T. However, at higher temperatures and especially at T close to T_c the -3 dB roll-off frequency increases dramatically. For two samples (Sp2 No. 17 and MgO3 No. 11) the spectra of the response obtained at the highest operating temperatures were flat within the accuracy of the measurements. Therefore, the last points for these samples, indicated by open symbols on the graph, are plotted at the maximal IF of about 25 GHz.

Figure 6 shows that the low-temperature values of $f_{\rm ro}$ greatly change from sample to sample. The difference is more than an order of magnitude if we compare sample MgO17 No. 10 [$f_{\rm ro}(T/T_c=0.1)\approx 7.5$ GHz] and samples MgO4 No. 3 and MgO4 No. 5 [$f_{\rm ro}(T/T_c=0.9)\approx 0.3$ GHz]. In analyzing these results we have found that samples with a higher normal state resistivity ρ_n (see Table I) show higher values of $f_{\rm ro}$ at low temperatures. For example, among samples Sp2 No. 11, Sp2 No. 17, and MgO3 No. 11 the normal state resistivity of the first one has the smallest value

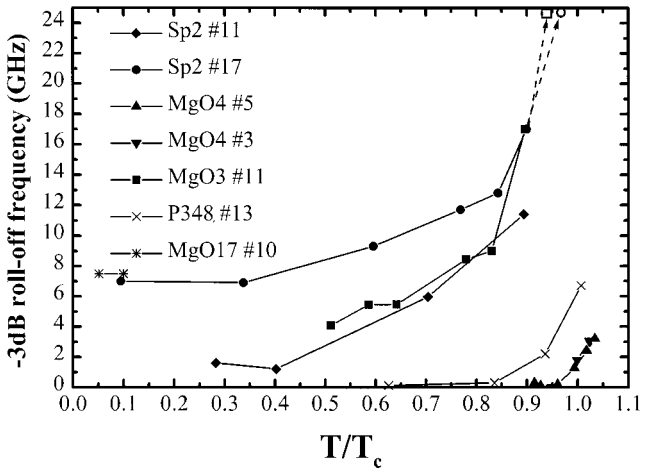

FIG. 6. Temperature dependence of the -3 dB roll-off frequency $f_{\rm ro}$ measured at $U_{\rm bias}<U_0$. Open symbols show the value of $f_{\rm ro}$ for samples Sp2 No. 17 and MgO3 No. 11 measured at the highest operating temperature, where the spectra of the response have no clearly detected -3 dB drop of the signal. The lines are to guide the eye.

($\approx 450\ \Omega$ cm), ρ_n of Sp2 No. 17 is the largest ($\approx 940\ \Omega$ cm), and ρ_n of the sample MgO3 No. 11 has an intermediate value of about 685 Ω cm. The magnitudes of the -3 dB roll-off frequency at $T/T_c\approx 0.5$ are 2.7, 4, and 8.5 GHz for samples Sp2 No. 11, MgO3 No. 11, and Sp2 No. 17, respectively. It is also possible to find similar dependence of the roll-off frequency for samples with larger thicknesses (P348 No. 13 and MgO4 No. 5), but only at temperatures close to T_c: an increase of the resistivity leads to an increase of the roll-off frequency at a given temperature.

An additional correlation was observed between the -3 dB roll-off frequency and the upper critical magnetic field $H^*_{c2}(0)$ evaluated from the experimentally determined value of the temperature derivative of the second critical magnetic field $dH^*_{c2}(T)/dT$. Some of our samples (Sp2 No. 11, Sp2 No. 17, MgO17 No. 10, and MgO3 No. 11) are characterized by a small value of $H^*_{c2}(0)$ in comparison with the others. For example, for a sample on sapphire Sp2 No. 11 the value of $H^*_{c2}(0)$ is two times smaller than for MgO4 No. 5 (see Sec. II). At the same time, these samples with lower value of $H^*_{c2}(0)$ demonstrate a higher $f_{\rm ro}$ value over the whole temperature range.

Before we start discussion of the results obtained we will repeat the basic experimental facts concerning the -3 dB roll-off frequency of the response of the YBCO thin-film microbridge to electromagnetic radiation.

(1) We have found a characteristic bias voltage U_0, which corresponds to the first maximum of the differential resistance of the YBCO thin-film microbridge. At voltages higher than U_0 the response spectrum has a -3 dB roll-off frequency, which corresponds to the frequency $f_{\rm es}=(2\pi\tau_{\rm es})^{-1}$ of the phonon escape from the film to the substrate. At $U_{\rm bias}<U_0$ the $f_{\rm ro}$ value is larger than $f_{\rm es}$ and decreases gradually as the bias voltage approaches U_0.
(2) The -3 dB roll-off frequency measured at $U_{\rm bias}>U_0$ has no detectable temperature dependence, since the intermediate frequency dependence of the YBCO microbridge response at this bias condition is caused by phonon escape from the film to the substrate.
(3) Measurements of the -3 dB roll-off frequency performed at $U_{\rm bias}<U_0$ show an increase of the $f_{\rm ro}$ value with an increase in operating temperature.
(4) YBCO thin-film microbridges characterized by higher resistivity and lower value of the upper critical magnetic field reveal a higher value of the -3 dB roll-off frequency measured at $U_{\rm bias}<U_0$ at certain operating temperatures.

The gradual transition of $f_{\rm ro}$ from a large value at $U_{\rm bias}<U_0$ to a smaller one at voltages above U_0 can be explained by the simultaneous presence and competition of two different mechanisms of the response of the YBCO bridge on electromagnetic radiation: heating of electrons and phonons and vibration of magnetic vortices. A change in bias voltage gives rise to more favorable conditions for one or the other mechanism, which then becomes dominant and determines the response of a microbridge. Because of different charac-

teristic response times of these mechanisms and depending on their relative contribution to the response at a given bias voltage we obtain a lower or higher -3 dB roll-off frequency. The temperature dependence of f_{ro} and the difference in its low-temperature values for different samples are explained by the same approach.

Heating of electrons in superconductors is a well-known effect and we refer the reader to a review[13] for a detailed description. Now let us consider the second mechanism that contributes to the response of a YBCO thin-film microbridge. Transport current flows through the microbridge and creates magnetic vortices that penetrate the microbridge. Under the influence of Lorenz force these vortices move across the microbridge and create an electric field directed along the bridge. Under external electromagnetic radiation there is additional force, which acts on vortices and results in their vibration near the quasiequilibrium state. In the presence of two radiation sources with close radiation frequency vortices vibrate with a periodically changing amplitude. The beating frequency of the vibration amplitude is $\Delta f=|f_{LO}-f_S|$, where f_S is the radiation frequency of the signal source. The vibration of magnetic vortices with velocity $\nu_V(t)$ (the amplitude of the velocity is also modulated with the same frequency Δf) creates an alternating electric field,

$$E(t)=\nu_V(t)B(I_{tr}), \tag{2}$$

where $B(I_{tr})$ is the magnetic induction created by the transport current. The equation of motion of the magnetic vortex could be written in the form of constrained vibrations with damping,

$$m\ddot{x}=-kx-\eta\dot{x}+F_1(t)+F_2(t), \tag{3}$$

where x is the displacement and m is the mass of the vortex, k and η are the pinning and viscous drag coefficients, respectively, $F_1(t)$ and $F_2(t)$ are two external forces induced by the local oscillator and signal sources. Solving Eq. (3) with regard to $\nu_V=\dot{x}$ we obtain the swing of the beating amplitude of the velocity,

$$\Delta A_V=\max A_V-\min A_V, \tag{4}$$

and its dependence on intermediate frequency in the following form:

$$\Delta A_V(\Delta\omega)\propto\frac{2F_2(\omega_{LO}+\Delta\omega)}{m\sqrt{[\omega_0^2-(\omega_{LO}+\Delta\omega)^2]^2+\lambda^2(\omega_{LO}+\Delta\omega)^2}}. \tag{5}$$

In Eq. (5) $\omega_0\equiv 2\pi f_0$ is the fundamental frequency of an oscillator $\sqrt{k/m}$, λ is the viscosity of a medium $\eta/2m$, and $\Delta\omega\equiv 2\pi\Delta f$ is the intermediate circular frequency. The temperature dependencies of f_0 and λ are determined by the temperature dependencies of the pinning constant k and of the viscous drag coefficient η, which can be written according to Ref. 15 as

$$k\propto H_c^2(0)(1-t)^{4/3}(1+t)^2, \tag{6}$$

$$\eta\propto\frac{H_{c2}(0)}{\rho_n}\frac{1-t^2}{1+t^2}, \tag{7}$$

where $t=T/T_c$ is the reduced temperature, and $H_c(0)$, $H_{c2}(0)$ are the thermodynamic and upper critical magnetic field, respectively. In Ref. 16 the mass of the magnetic vortex was determined to be proportional to η^2.

We would like to note that all our experimentally measured spectra have no specific features which could be identified as a resonant peak. In the case of $f_{LO}<f_0$ the beating amplitude of the velocity ΔA_ν, Eq. (5), will have resonance at $\Delta f=f_0-f_{LO}$. A typical experimental response spectrum has a plateau at low intermediate frequencies and gradually decreases at higher IF until the highest frequencies of measurements. We also estimated the fundamental frequency f_0 using the most frequently occurring values in the literature of the pinning constant and the viscous drag coefficient. For $k\approx 10^5$ N/m^2 and $\eta\approx 10^{-6}$ N s/m^2 (see, for example, Ref. 15) f_0 will be about 0.5 GHz, which is much smaller than our local oscillator frequency of 100 GHz. Thus, we will now consider only the high-frequency limit, i.e., $f_{LO}>f_0$, where the spectrum of the response is monotonic and can be described by a reduced formula,

$$\Delta A_V(\Delta f)\approx\frac{2F_2}{m(f_{LO}+\Delta f)}, \tag{8}$$

with the characteristic roll-off frequency $\Delta f\approx 0.4f_{LO}$.

Taking into account all arguments stated before the total response of the YBCO bridge, in the general case can be written as

$$\Delta U(\Delta f)=W_V\times\Delta U_V(\Delta f)+\Delta U_{es}(\Delta f), \tag{9}$$

where W_V is a phenomenological factor dependent on the YBCO film quality and operating conditions. $\Delta U_V(\Delta f)$ and $\Delta U_{es}(\Delta f)$ are the contributions from vibrating vortices and hot electrons calculated using Eqs. (5) and (1), respectively. At U_{bias} higher than the voltage of the FMDR hot-spot formation prevents magnetic vortex penetration into a bridge, thus the vortex contribution to the response is negligible and we suppose $W_V=0$. The total response is only due to heating of electrons in the film, and the -3 dB roll-off frequency in our relatively thick films is determined by the phonon escape time. In this case there is no temperature dependence of f_{ro}, which is in good agreement with our experimental results. The situation at $U_{bias}<U_0$ is nontrivial substantially. Within this limit the factor W_V is nonzero and its absolute value is determined by a lot of parameters.

To simplify the problem we make some assumptions. In principle, we have to take into account the influence of the transport current value on the magnitude of the vortex contribution [see Eq. (2)]. At the same bias voltage the higher the temperature the lower the transport current that flows through the YBCO bridge and as a result this current induces a smaller magnetic field. At the same time the hot-electron contribution is also proportional to the transport current,

$$\Delta U_{es}(0)\propto I\times\Delta R=I\frac{dR}{dT}\Delta T. \tag{10}$$

Since the magnitudes of both contributions are proportional to the transport current we can assume that this transport-current factor is more or less the same for both and ignore it in further considerations.

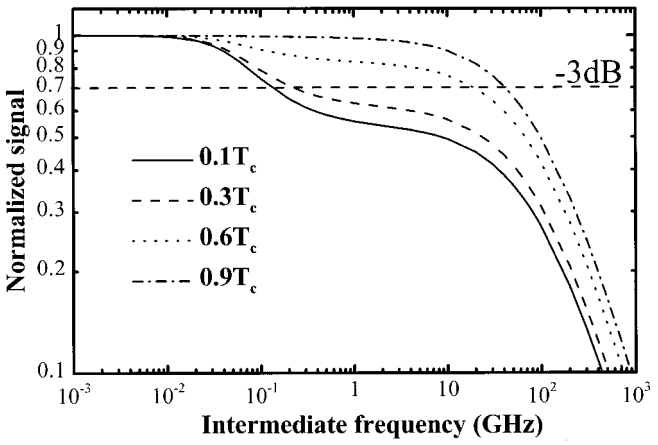

FIG. 7. Simulated dependence of the response of a YBCO thin-film microbridge on the intermediate frequency calculated for several operating temperatures. The response is normalized to the value at zero intermediate frequency. The dashed horizontal line indicates the −3 dB level of the response drop.

At the same time it is clearly seen from Eq. (8) that $\Delta U_V(0) \propto m^{-1}$ and strongly increases as the temperature approaches T_c. Thus, for our calculations we can suppose that the magnitude of the hot-electron contribution at least remains the same but the vortex response increases with the temperature due to reduction of $m \sim \eta^2$, Eq. (7). Figure 7 shows the normalized curves of the total response of the microbridge calculated at different temperatures and for a certain value of W_V using Eq. (9). The dashed horizontal line indicates the position of the −3 dB drop of the signal. The broadening of the spectrum with an increase in temperature is seen clearly. Also, from our calculations we obtain changes in the shape of the spectrum. At $T=0.1T_c$ it is characterized by two plateaus: the first is due to phonon escape with −3 dB rolloff at $\Delta f \approx 100$ MHz and the second one is attributed to the vortex mechanism. At temperature $T=0.6T_c$ the vortex contribution to the microbridge response becomes larger, the difference between these two plateaus is already less than 3 dB, and $f_{ro} \approx 20$ GHz is determined almost completely by the vortex vibration mechanism.

In Fig. 8 we present results of our calculations of the

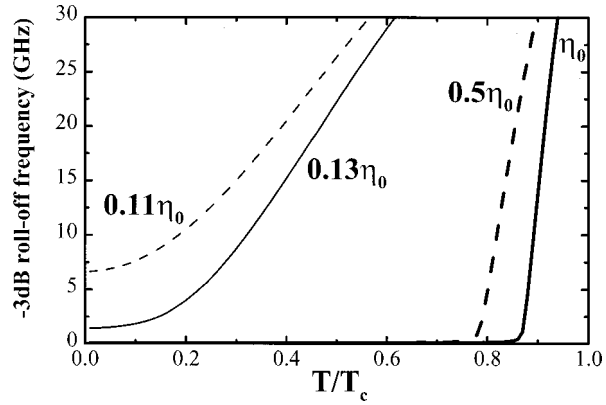

FIG. 8. Dependence of the −3 dB roll-off frequency on the reduced temperature calculated for different values of viscous drag coefficient η indicated near each curve.

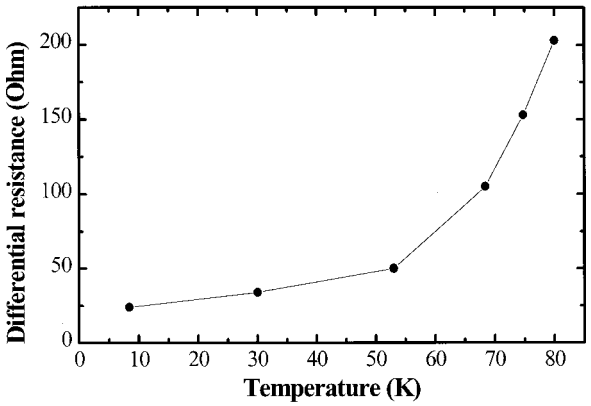

FIG. 9. Experimental dependence of differential resistance at $U_{bias} \to 0$ on the operating temperature for sample Sp2 No. 17. The line is to guide the eye.

dependence of the −3 dB roll-off frequency on reduced temperature for different values of the viscous drag coefficient η. It is seen that the theoretically obtained picture (Fig. 8) looks qualitatively similar to the experimental results (Fig. 6). Without any additional assumptions we have obtained from Eq. (9) an increase of f_{ro} with an increase in operating temperature. We have found that the larger vortex contribution to the microbridge response leads to the higher −3 dB roll-off frequency at certain T. The increase of the vortex contribution can be simulated either by increasing factor W_V or by reducing η. The results of calculations shown in Fig. 8 were obtained by varying the viscous drag coefficient only. These variations reflect changes of the upper critical magnetic field and of the film resistivity, Eq. (7), simultaneously. The two curves on the left ($0.11\ \eta_0$ and $0.13\ \eta_0$) were obtained for values of η which are about four to eight times smaller than those for the curves on the right ($0.5\ \eta_0$ and η_0). We have to note that for a lower value of η the −3 dB roll-off frequency dependencies on T are more sensitive to changes of η than for higher values. The values of η for the pair of curves on the left (solid and dashed lines) differ from one another by less than by 20%. At the same time, we have changed η by a factor of 2 to reach the difference for the curves on the right (solid and dashed lines) in Fig. 8, which describes more or less the experimental situation.

The calculated temperature dependencies of the −3 dB roll-off frequency are stronger than the experimental dependencies. One of the reasons is the presence of the additional damping factor, which weakens the vortex contribution to the total response. As seen in Fig. 9 the differential resistance of sample Sp2 No. 17 at $U_{bias}=0$ is nonzero and depends on the temperature. This means that at a given T and even at voltages much lower the FMDR the microbridge already contains some regions in the normal state. These regions grow with the temperature and interfere with motion of the magnetic vortices. This effect can, in principle, strongly suppress the vortex contribution in the total response of the YBCO thin-film microbridge to electromagnetic radiation.

The recently reported dependence of the IF bandwidth of the HTS HEB mixer on the frequency of radiation[8] can be found within the framework of our theoretical approach also.

The value of the vortex contribution in the response of the YBCO bridge is inverse to the local oscillator frequency, Eq. (8). So, at terahertz LO frequency the vortex response of the YBCO microbridge will be at least 10 times weaker than at 100 GHz and the -3 dB roll-off frequency can be completely determined by the hot-electron contribution. At the same time the HEB mixer bandwidth about 7 GHz obtained at 585 GHz LO frequency[7] is evidence of the dominant effect of the vortex contribution in the mixer response even at six times higher LO frequency than in the present study. We have obtained the same f_{ro} of about several gigahertz for two values of f_{LO} (1 and 0.1 THz) using for calculations at higher f_{LO} a three times smaller η value than for $f_{LO}=0.1$ THz. This means that in the YBCO thin films characterized by low magnitude of the upper critical magnetic field and high normal-state resistivity vortex motion can play an appreciable role in the determination of the microwave response of the microbridge.

V. CONCLUSION

The dependencies of the -3 dB roll-off frequency on the operating temperature, bias voltage, and YBCO film quality were studied experimentally and theoretically. It was shown that these phenomena could be explained by the competition of two additive mechanisms of the response of a YBCO thin-film microbridge to the electromagnetic radiation. The first mechanism, the so-called heating of electrons and phonons, dominates the response of a sample at bias voltages higher than the voltage, which corresponds to the first maximum of the differential resistance and also at temperatures much smaller than T_c. The last assertion is true only for films characterized by a high value of the second critical magnetic field and low resistivity. On the other hand, YBCO high resistivity samples with low viscous drag coefficient have a -3 dB roll-off frequency value of about several gigahertz even at $T \ll T_c$. This huge magnitude of f_{ro} is due to the second mechanism of the response: vibration of magnetic vortices. The competition between these two mechanisms determines the temperature, bias voltage, and film quality dependencies of the -3 dB roll-off frequency of YBCO thin-film microbridge response to microwave electromagnetic radiation. We believe that even in the terahertz frequency range the devices made from the YBCO thin films with high normal-state resistivity and small value of upper critical magnetic field could be used for detecting and mixing radiation using the effect of magnetic vortex vibration. Further experimental and theoretical studies of the magnetic vortex contribution to the microwave response of the YBCO bridge are needed, especially those that focus on nonlinearity, which occurs at large amplitude of the signal, and also a detailed study of vortex vibration at high local oscillator frequency in the terahertz range.

ACKNOWLEDGMENTS

This work was partly supported by BMBF Project No. 13N7321/6. The authors are grateful to Oliver Harnack for establishing and automatizing the experimental setup.

[1] B. S. Karasik, W. R. McGrath, and M. C. Gaidis, J. Appl. Phys. **81**, 1581 (1997).
[2] M. Danerud, D. Winkler, M. Lindgren, M. Zorin, V. Trifonov, B. S. Karasik, G. N. Gol'tsman, and E. M. Gershenzon, J. Appl. Phys. **76**, 1902 (1994).
[3] M. Lindgren, V. Trifonov, M. Zorin, M. Danerud, D. Winkler, B. S. Karasik, G. N. Gol'tsman, and E. M. Gershenzon, Appl. Phys. Lett. **64**, 3036 (1994).
[4] A. D. Semenov, R. S. Nebosis, Yu. P. Gousev, M. A. Heusinger, and K. F. Renk, Phys. Rev. B **52**, 581 (1995).
[5] M. Lindgren *et al.*, Appl. Phys. Lett. **74**, 853 (1999).
[6] A. V. Sergeev, A. D. Semenov, P. Kouminov, V. Trifonov, I. G. Goghidze, B. S. Karasik, G. N. Gol'tsman, and E. M. Gershenzon, Phys. Rev. B **49**, 9091 (1994).
[7] C.-T. Li, B. S. Deaver, Jr., M. Lee, R. M. Weikle II, R. A. Rao, and C. B. Eom, Appl. Phys. Lett. **73**, 1727 (1998).
[8] O. Harnack, K. S. Il'in, M. Siegel, B. S. Karasik, W. R. McGrath, and G. de Lange, Appl. Phys. Lett. **79**, 1906 (2001).
[9] O. Harnack, B. Karasik, W. McGrath, A. Kleinsasser, and J. Barner, Semicond. Sci. Technol. **12**, 850 (1999).
[10] M. E. Lopez-Morales, D. Rios-Jara, J. Tagüena, R. Escudero, S. La Placa, A. Bezinge, V. Y. Lee, E. M. Engler, and P. M. Grant, Phys. Rev. B **41**, 6655 (1990).
[11] The operating temperature range is from 30 mK to 300 K with a magnetic field up to 2 T. The thermal stability is better than 0.1 K at temperatures of about 70 K.
[12] F. Arams, C. Allen, B. Peyton, and E. Sard, Proc. IEEE **54**, 612 (1966).
[13] A. V. Sergeev and M. Yu. Reizer, Int. J. Mod. Phys. B **10**, 635 (1996).
[14] M. Tinkham, *Introduction to Superconductivity*, 2nd ed. (McGraw–Hill, New York, 1996).
[15] M. Golosovsky, M. Tsindlekht, and D. Davidov, Semicond. Sci. Technol. **9**, 1 (1996).
[16] S. Grundberg and J. Rammer, Phys. Rev. B **61**, 699 (2000).